

## Optimal Operation of Photovoltaic System with a DC-DC Boost Converter FED SAF Using ICos $\phi$ Algorithm

G.Vijayakumar<sup>1\*</sup> and R.Anita<sup>2</sup>

<sup>1</sup>Department of Electrical and Electronics Engineering, K.S.R. College of Engineering, Tiruchengode – 637215, Tamil Nadu, India

<sup>2</sup>Department of Electrical and Electronics Engineering, Institute of road and transport technology, Erode, Tamil Nadu, India

Received 4 January 2014; Accepted 21 July 2014

### Abstract

This paper presents an optimal utilization of Photovoltaic (PV) solar system based Shunt Active Filter (PV-SAF) for harmonic mitigation, real and reactive power compensation at the point of common coupling (PCC) throughout the day. This PV system operated SAF reduces the energy consumption by disconnecting the utility grid from the load through semiconductor switches, when the PV system generates excessive or equal real power to the required load demand. However, the reduction of energy consumption is always desirable for the reduction of panel tariff and global warming gasses. The PV module is connected to the DC side of SAF through the DC-DC converter with fuzzy based Perturb & Observe (P&O) Maximum Power Point Tracking (MPPT) algorithm to eliminate the drawback of the conventional PV system by tracking maximum power point of the PV array is presented. The reference currents extract by the Fuzzy logic controller based ICos $\phi$  control strategy. This proposed PV-SAF, if connected at the terminals of a small industry or a home or a small enlightening institution can avoid interruptible power supply, use of individual stabilizer and potential panel tariff over a 12 hour period. A MATLAB simulink is presented to validate the advantage of the proposed system.

*Keywords:* Shunt Active Filter (PV-SAF), P&O MPPT, DC-DC converter, Energy conservation.

### 1. Introduction

Recently, the usage of the sensitive loads such as computers, medical equipment and devices in Information Technology are increased, it is operated continuously during a 24 hours period and requires reliable power supply. If supplying unreliable power these devices bring severe losses to the domestic and industrial customers. Then again, increase the EMI problem, real and reactive power losses which cause harmonics phenomena on the line current. So the power qualities become more important to maintain the safety of electrical devices and customer satisfaction.

The proposed PV-SAF is connected in shunt with the three-phase distribution system. The VSI based SAF injects current of the same amplitude and reverse phase to that of the load current into the ac system, in order to compensate the source current. The DC-link voltage is decreasing during the compensation. The SAF supported DC-link capacitor consumes more power from the distribution system for the continuous compensation. Taking these aspects into account, renewable power generation system integrated with SAF is proposed in this work. The PV-SAF is proposed for source current harmonic reduction, supply of real and reactive power to the load and satisfies the load demand. The interfacing inductor provides the isolation and filtering between the three-leg VSI and the distribution system.

At present, the nations have increased the use of PV system in the power system application. PV-SAF system has become favorable solutions for frequent power interruptions in a day. This may occur in the developing countries, where

the generated electrical power is less than their demand. PV power generation systems have the disadvantage that the PV array loses the output capability, when the irradiation level changes. In order to attain the maximum power point of a PV array, a simple DC-DC converter associated with a function called MPPT is introduced between the PV array and battery bank.

ICos $\phi$  control algorithm is attractive that the control scheme should be applicable in any practical power system under the operating conditions such as balanced source/load and unbalanced source/load. In the frequency domain, the device switching frequency of the SAF is kept generally more than twice the highest compensating harmonic frequency for effective compensation<sup>1</sup>. Correction in the time domain is based on the principle of holding the instantaneous values within some reasonable tolerances. An instantaneous error function is computed on-line, which is the difference between actual and reference current/voltage waveform. The greatest advantage of time domain correction is its fast response to changes in power system. It is easy to implement and has very little computational burden. In the time domain the most commonly used methods that present a good dynamic response are based on Instantaneous Reactive Power Theory (IRPT), Synchronous Detection (SD), DC bus voltage algorithm or ICos $\phi$  algorithm. Akagi<sup>2</sup> introduced IRPT, which is widely discussed because of its fast dynamic response.

The advantages of fuzzy logic controllers over the conventional PI controller are that they do not need an accurate mathematical model; they can work with imprecise inputs, can handle nonlinearity, and may be more robust than the conventional PI controller. The Mamdani type of fuzzy controller used for the control of SAF gives better results

\* E-mail address: vijayakumargovind@yahoo.com

compared with the PI controller, but it has the drawback of a larger number of fuzzy sets and 49 rules<sup>3</sup>. Though several control techniques and strategies had developed but still performance of the filter in contradictions<sup>4</sup>, these became a primary motivation for the current paper. The Present paper focusing the performance of the on fuzzy controller, in addition to developing a filter with ICosΦ control strategy which is prominent one to analyze the performance of filter under different voltages. To validate current observations, Extensive simulations were performed and the detailed simulation results are included.

**2. System configuration**

The power circuit of the proposed PhotoVoltaic system based SAF topology namely PV-SAF is presented. The PV-SAF is designed to compensate the current disturbance at the load side. It is also designed to inject the real power generated by the PV system to load on whole day. When the PV system generates is less power than the load demand and the proposed logic connects the three phase rectifier output in parallel with the DC capacitor to share the load demand. The PV-SAF consists of PV array, rectifier, converter, energy storage unit, VSI, filters and switches S<sub>1</sub>, S<sub>2</sub>, S<sub>3</sub>, P<sub>1</sub>, P<sub>2</sub>, P<sub>3</sub> and R<sub>1</sub>, R<sub>2</sub>. The proposed circuit topology of the three phase PV-SAF is shown in Fig.1.

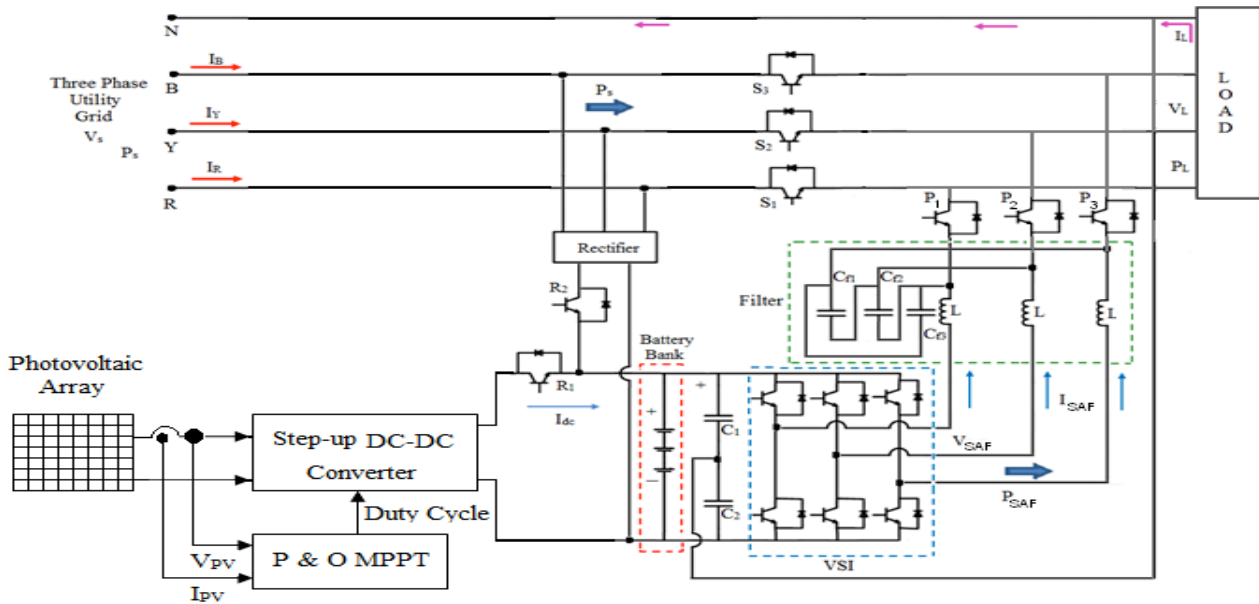


Fig.1. Block diagram of the proposed PV-SAF

The proposed 3-phase PV-SAF operates in two modes as in Table 1: 1) compensation mode and 2) UPS Energy conservation mode. In the first mode, under normal condition the semiconductor S<sub>1</sub>, S<sub>2</sub>, S<sub>3</sub> switches are turned ON and R<sub>1</sub>, R<sub>2</sub> turned OFF. When SAF detects difference in the current, then the SAF enter into compensation mode through the inductor. 3phase AC current is injected in shunt with desired magnitude, phase angle and wave shape for the compensation. In the second mode, when the PV system generates excessive or equal real power to the load demand, then the SAF enters into a UPS energy conservation mode. The system aims to transfer the power generated on the PV system to the AC load through the three-phase VSI. The excessive power generation of the PV system, turns ON the switch R<sub>1</sub> and turns OFF the switch R<sub>2</sub>. During this mode, the switches S<sub>1</sub>, S<sub>2</sub>, S<sub>3</sub> are turned OFF and the switches P<sub>1</sub>, P<sub>2</sub> and P<sub>3</sub> are turned ON as presented in Table 2.

Table 1. Control signals for S<sub>1</sub>, S<sub>2</sub>, S<sub>3</sub>, P<sub>1</sub>, P<sub>2</sub>, P<sub>3</sub> and R<sub>1</sub>, R<sub>2</sub>.

Mode	Control Signals					
	S <sub>1</sub>	S <sub>2</sub>	S <sub>3</sub>	P <sub>1</sub>	P <sub>2</sub>	P <sub>3</sub>
Compensation	1	1	1	0	0	0
UPS Energy Conservation	0	0	0	1	1	1

Table 2. Battery charge control

Condition	Control Signals		Battery Charging Unit
	R1	R2	
P <sub>PV</sub> ≥ P <sub>L</sub>	1	1	PV system
P <sub>PV</sub> < P <sub>L</sub>	0	0	PV system & Rectifier

**3. Detection of disturbance**

According to ICosΦ algorithm, the source is required to supply only the real part of the fundamental component of the load current. Remaining parts of load current i.e., reactive component and harmonics are to be supplied by the active filter. Assuming a balanced source, the three phase instantaneous fundamental component of voltages can be represented by<sup>5</sup>

$$v_a = V_m \sin \omega t; v_b = V_m \sin(\omega t - 120^\circ); v_c = V_m \sin(\omega t - 240^\circ) \tag{1}$$

Where, a, b, c is phases a, b, c, respectively, V<sub>m</sub> is peak value of the instantaneous voltage, i<sub>L</sub> is instantaneous load current in phases a, b, c, respectively. The fundamental component of the load current is separated with the help of

biquad low pass filter. Its output is fundamental component is delayed by  $90^\circ$  during the filtering operation.

$$i_{Lfa} = I_{La.1} \sin(\omega t - \phi_{1a} - 90^\circ) \quad (2)$$

$$i_{Lfb} = I_{Lb.1} \sin(\omega t - \phi_{1b} - 120 - 90^\circ) \quad (3)$$

$$i_{Lfc} = I_{Lc.1} \sin(\omega t - \phi_{1c} - 120 - 90^\circ) \quad (4)$$

The real part of the fundamental component of load current is estimated as follows: At the time of negative zero crossing of the input voltage of any one phase, say a phase, i.e., at  $\omega t = n\pi$ , instantaneous value of fundamental component of load current is the peak value of real component of the fundamental load current. Similarly, instantaneous values of fundamental components of phase b load current at  $\omega t = 300^\circ$  and phase c load current at  $\omega t = 60^\circ$  are the respective real components. The magnitude of the desired source current  $|I_{s(ref)}|$  is the magnitude of real part of the fundamental component of load current in the respective phases, i.e., for phase a it can be written as  $|I_{s(ref)}| = |\text{Re}(I_{La})|$ . To ensure balanced, sinusoidal, unity power factor currents to be drawn from the source, the magnitude of the desired source current can be expressed as the average of the magnitudes of the real components of the fundamental load currents in the three phases.

$$|I_{s(ref)}| = \frac{|\text{Re}(I_{La})| + |\text{Re}(I_{Lb})| + |\text{Re}(I_{Lc})|}{3} \quad (5)$$

$$|I_{s(ref)}| = \frac{|I_{La}| \cos \phi_a + |I_{Lb}| \cos \phi_b + |I_{Lc}| \cos \phi_c}{3} \quad (6)$$

The voltage fluctuations in DC bus voltage of active filter are also sensed and given to fuzzy controller, which calculates the current to be taken from the source to meet power loss in the inverter and coupling inductor. This current is added to the average value of  $|I_{s(ref)}|$ . The three phase source voltages are used as templates to generate unit amplitude sine waves in phase with source voltages and they are expressed as,

$$U_a = 1 \sin \omega t \quad (7)$$

$$U_b = 1 \sin(\omega t - 120^\circ) \quad (8)$$

$$U_c = 1 \sin(\omega t - 240^\circ) \quad (9)$$

The desired (reference) source currents in the three phases are obtained by multiplying reference source currents with unit amplitude templates of the phase to ground source voltages in the three phases respectively.

$$i_{sa(ref)} = |I_{s(ref)}| * U_a = |I_{s(ref)}| \sin \omega t \quad (10)$$

$$i_{sb(ref)} = |I_{s(ref)}| * U_b = |I_{s(ref)}| \sin(\omega t - 120^\circ) \quad (11)$$

$$i_{sc(ref)} = |I_{s(ref)}| * U_c = |I_{s(ref)}| \sin(\omega t + 120^\circ) \quad (12)$$

The compensation currents to be injected by the shunt active filter are the difference between the actual load currents and the desired source currents. The equivalent block diagram of  $I_{cos\phi}$  algorithm is shown in Fig.2.

$$i_{a(comp)} = i_{La} - i_{sa(ref)}; i_{b(comp)} = i_{Lb} - i_{sb(ref)}; i_{c(comp)} = i_{Lc} - i_{sc(ref)} \quad (13)$$

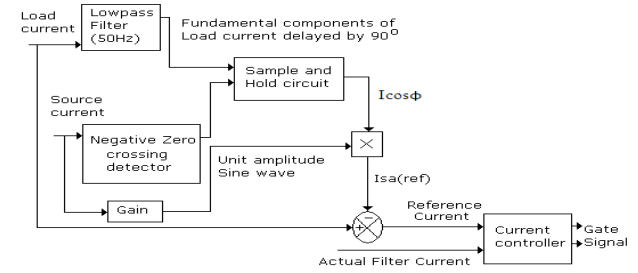


Fig.2. Block diagram of  $I_{cos\phi}$  algorithm for a phase

#### 4. PV- SAF site selection

Table 3 shows the average temperature and solar radiation variations at Erode district, Tamil Nadu, India for a period of 15 days. These data are collected from Tamil Nadu Agricultural University, Coimbatore<sup>6</sup> to estimate the possible output of the PV array. From Table 3, it is observed that the location is well endowed with solar resources, which favors the use of solar conversion system in the selected area.

Table 3. Erode weather data

Date	Air Temp. ( $^\circ\text{C}$ )		Solar Radiation ( $\text{cal/cm}^2$ )
	Max	Min	
01.06.2013	30.6	23.5	243.53
02.06.2013	30.1	23.8	270.79
03.06.2013	31.9	21.9	326.29
04.06.2013	30.8	23.7	377.34
05.06.2013	31.7	22.3	304.93
06.06.2013	32.0	20.1	379.48
07.06.2013	31.9	20.4	457.73
08.06.2013	30.9	19.2	410.80
09.06.2013	30.5	20.2	299.62
10.06.2013	32.5	21.4	390.92
11.06.2013	31.5	21.4	360.82
12.06.2013	32.9	21.3	418.46
13.06.2013	32.4	21.1	386.14
14.06.2013	32.2	23.0	379.54
15.06.2013	32.7	21.0	402.72
<b>Average</b>	<b>31.1</b>	<b>20.3</b>	<b>360.82</b>

#### PV array modeling

PV arrays are built up with combined series/parallel combinations of PV solar cells. The PV array requires DC-DC converter to regulate the output voltage under the sudden changes in weather conditions as shown in Table 3, which change the solar irradiation level as well as cell operating temperature. An equivalent circuit model of photovoltaic cell

with DC-DC converter is shown in Fig.3. The output voltage of the PV cell is a function of photo current that is mainly determined by load current depending on the solar irradiation level during the operation<sup>7</sup>. The PV cell output voltage is expressed as

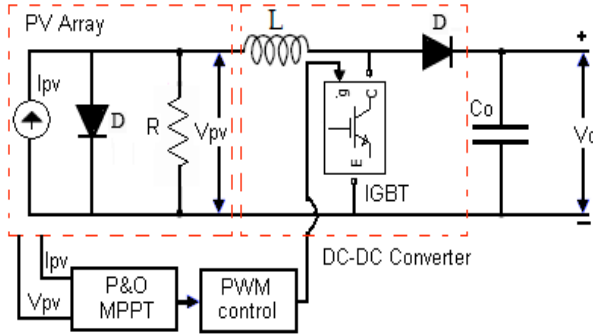


Fig.3. PV- boost with P&O MPPT algorithm

$$V_c = \frac{AkT_c}{e} \ln \left( \frac{I_{ph} + I_c - I_0}{I_0} \right) - R_s I_c \quad (14)$$

where, e is the charge of electron,  $V_c$  is the output voltage of PV cell in volts,  $I_{ph}$  is the photo current in A,  $I_0$  is the reverse saturation current of diode, k is Boltzmann constant ( $1.38 \times 10^{-23} J/K$ ),  $I_c$  is the cell output current in A,  $R_s$  is the cell internal resistance,  $T_c$  is the operating temperature of the reference cell 25 °C.

The design parameters  $I_{ph}$ ,  $I_0$ ,  $R_s$  and  $T_c$  are determined from the data sheet and I-V characteristics of the PV array<sup>8</sup>. The operating temperature of solar cell varies as a function of solar irradiation level and ambient temperature. The effect of change in ambient temperature and solar irradiation levels are represented in the model by the temperature coefficients  $C_{TV}$  and  $C_{TI}$ .

$$C_{TV} = 1 + \beta_T (T_a - T_x) \quad (15)$$

$$C_{TI} = 1 + \frac{\gamma_T}{S_y} (T_x - T_a) \quad (16)$$

where,  $\beta_T = 0.004$  and  $\gamma_T = 0.06$ .  $T_a$  and  $T_y$  represent the ambient temperature of the cell and atmosphere.

The change in the operating temperature and in the photocurrent due to variation in the solar irradiation level can be expressed via two constants,  $C_{SV}$  and  $C_{SI}$ , which are the correction factors for changes in cell output voltage  $V_c$  and photocurrent  $I_{ph}$ , respectively:

$$C_{SV} = 1 + \beta_T \alpha_s (S_x - S_c) \quad (17)$$

$$C_{SI} = 1 + \frac{1}{S_c} (S_x - S_c) \quad (18)$$

Where,  $S_c$  is the benchmark reference solar irradiation level during the cell testing to obtain the modified cell model.  $S_x$  is the new level of the solar irradiation. The change in temperature can be expressed as,

$$\Delta T_c = \alpha_s (S_x - S_c) \quad (19)$$

Using correction factors  $C_{TV}$ ,  $C_{TI}$ ,  $C_{SV}$  and  $C_{SI}$ , the new values of the cell output voltage  $V_{cx}$  and photocurrent  $I_{phx}$  are obtained for the new temperature  $T_x$  and solar irradiation  $S_x$  as follows:

$$V_{cx} = C_{TV} C_{SV} V_c \quad (20)$$

$$I_{phx} = C_{TI} C_{SI} I_{ph} \quad (21)$$

A functional block diagram of photovoltaic (PV) array is shown in Fig.4. The mathematical model of a single PV cell is represented by equation 1. The effect of change in solar irradiation and temperatures are represented in the another block.

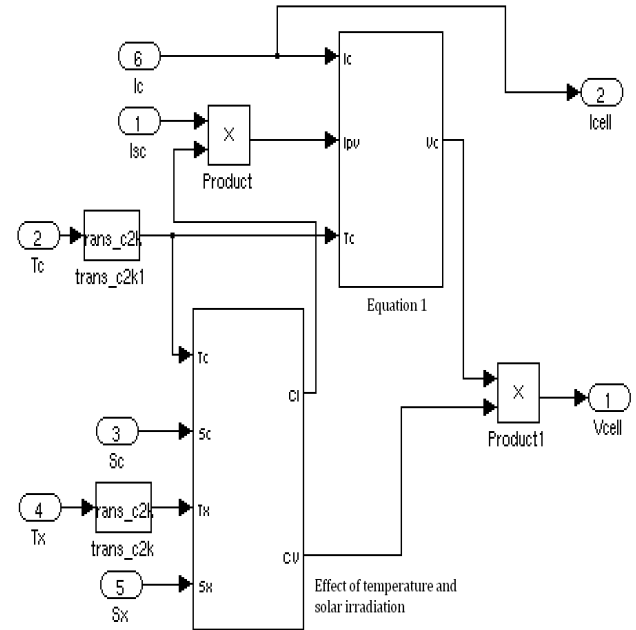


Fig.4. Functional of PV array block diagram.

The DC-DC boost converter as shown in the Fig.3. Is designed using the following basic equations<sup>9</sup>. The average output voltage of the converter is given as,

$$V_c = \frac{V_s}{1 - D} \quad \text{and} \quad D = \frac{T_{on}}{T_{on} + T_{off}} \quad (22)$$

where, D is the duty Cycle in %,  $T_{on}$  is on time of the switch,  $T_{off}$  is off time of the switch.

**Control method**

**PV array-MPP Tracking Method**

Currently the most popular MPPT algorithm is perturb and observe (P&O), where the current/voltage is repeatedly perturbed by a fixed amount in a given direction, and the direction is changed only if the algorithm detects a drop in power between steps. In the proposed work each perturbation of the controller gives a reference voltage which is compared with the instantaneous PV module output voltage and the error is fed to a fuzzy controller which in turns decides the duty cycle of the DC/DC converter. The process of perturbation is repeated periodically until the MPP is reached<sup>10</sup>.

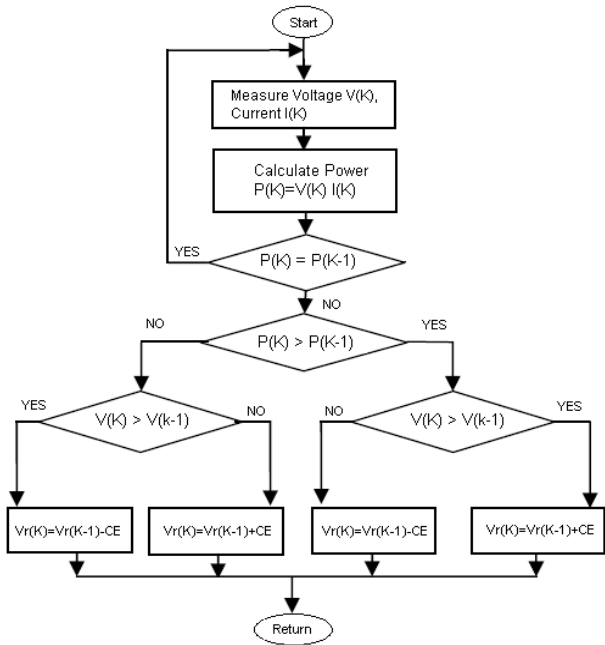


Fig.5. Flow chart of P&O MPPT algorithm

The computation of actual state ( $k$ ) and previous state ( $k-1$ ) of the parameters  $V$  and  $I$  are considered. The power is calculated from the product of actual and previous state  $V$  &  $I$ . According to the condition as represented in Fig.5, the increment or decrement of reference voltage of the PWM pulse generator is obtained. The simulink block diagram of the fuzzy controller based P&O MPPT is shown in Fig.6.

The inputs and output of fuzzy controller are expressed as a set of linguistic variables as follows: NB-Negative Big, NS-Negative Small, Z-Zero, PS-Positive Small and PB-Positive Big. The output of the fuzzy is chosen from a set of semantic rules that lead to track the maximum power point of PV array. The set of rules chosen are shown in Table 4.

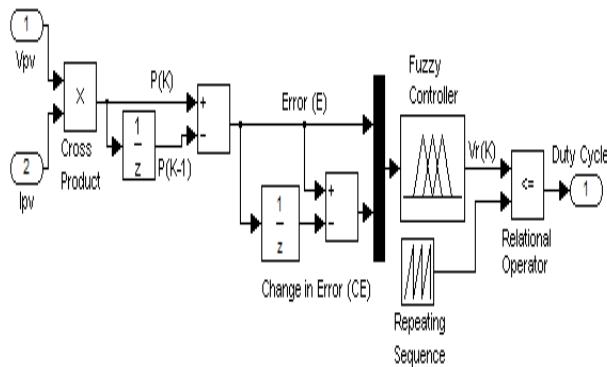


Fig.6. Control of fuzzy P&O MPPT

Table 4. Fuzzy rules for P&O MPPT

E/CE	NB	NS	ZE	PS	PB
NB	ZE	ZE	PB	PB	PB
NS	ZE	ZE	PS	PS	PS
ZE	PS	ZE	ZE	ZE	NS
PS	NS	NS	NS	ZE	ZE
PB	NB	NB	NB	ZE	ZE

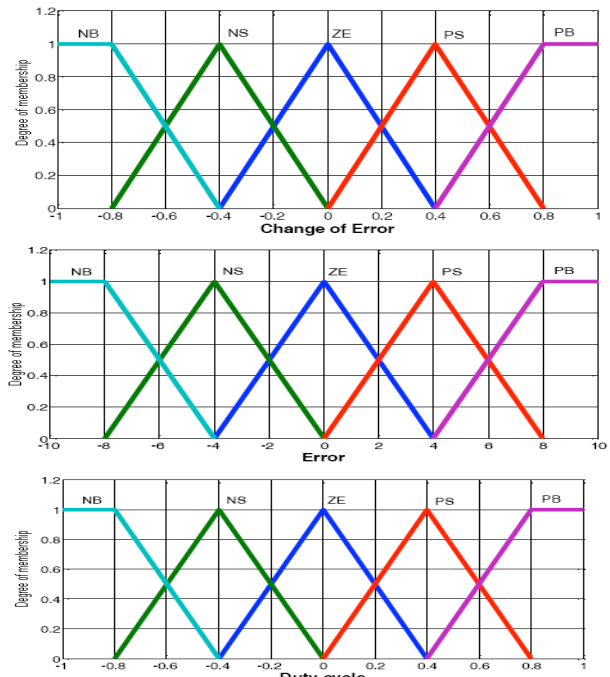


Fig.7. Membership function for E, CE & output

**SAF Controller**

The control system of SAF with fuzzy controller is shown in Fig.8. This compensator solves harmonic problems in the source side. In the conventional controllers like P, PI and PID, the control parameters are fixed at the time of design. Hence, the conventional controllers offer good performance only for the linear system. When the operating point of the system is changed, the parameters of the conventional controllers should be designed again, and some trials and prior information of the systems are needed to design the parameters. The fuzzy controller overcomes the drawbacks of the conventional controllers<sup>11-12</sup>.

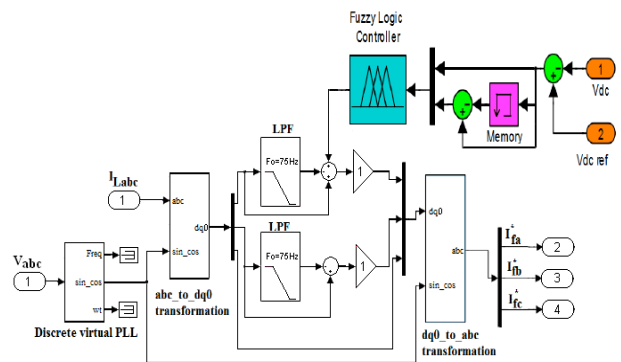


Fig.8. Control of SAF

The DC-bus voltage is first sensed and compared with DC reference voltage and error signal is generated. The error signal and its derivative are applied to fuzzy logic controller. Error signal is applied to “Memory” block and its output is subtracted from the error signal to obtain derivative of error signal as shown in the Fig.8. The processed error signal is modulated using Sinusoidal Pulse Width Modulation (SPWM) to produce the required pulse to switch on the three phase inverter, thus restoring the load voltage. To compare a sinusoidal frequency 50 Hz with a triangular carrier waveform  $V_{carrier}$  with 20 kHz signal to produce the PWM

pulses for three phase SAF. When the control signal is greater than the carrier signal, the switches are turned on, and their counter switches are turned off. The output voltage of the inverter mitigates harmonics.

The two inputs and the output use seven triangular membership functions namely Negative Big (NB), Negative Medium (NM), Negative Small (NS), Zero (ZE), Positive Small (PS), Positive Medium (PM), Positive Big (PB). The type and number of membership functions (MFs) decides the computational efficiency of a FLC. The shape of fuzzy set affects how well a fuzzy system of If-then rules approximate a function. The membership values of input and output variables are shown in the Fig.8. Each input has seven linguistic variables; therefore there are 49 input label pairs. A rule table relating each one of 49 input label pairs to respective output label is given in Table 5.

$$\text{Error (E)} = V_{\text{ref}} - |V_s| \tag{23}$$

$$\text{Change in Error (CE)} = E(n) - E(n - 1) \tag{24}$$

**Table 5.** Fuzzy rules for SAF control

E/CE	NB	NM	NS	ZE	PS	PM	PB
NB	PB	PB	PB	PM	PM	PS	ZE
NM	PB	PB	PM	PM	PS	ZE	NS
NS	PB	PM	PM	PS	ZE	NS	NM
ZE	PM	PM	PS	ZE	NS	NM	NM
PS	PM	PS	ZE	NS	NM	NM	NB
PM	PS	ZE	NS	NM	NM	NB	NB
PB	ZE	NS	NM	NM	NB	NB	NB

**5. Simulation results**

The performance of the proposed PV-SAF simulated under three cases. Balanced unbalanced source, balanced unbalanced nonlinear load and UPS energy conservation mode. Simulated results are presented for two cases. For these cases, the system frequency is maintained at 50 Hz and sample time is chosen to be 50 μsec. The input voltage of 400 V three-phase AC supply is given to load through three-phase programmable AC source. The switched-mode PWM VSI is made to operate at 180° conduction mode. Three-phase VSI is operated by six gate pulses generated from the PWM pulse generator. The PWM generator has pulse amplitude of 1V for all the six pulses. The system parameters considered for the analysis of the proposed PV-SAF are furnished in Table 6.

**Table 6.** PV-SAF simulated system

Parameter	Value
Nominal Line Voltage	400V
Frequency	50Hz
Load Resistance	360 Ω
Load Inductance	2 mH
Filter Inductance	40 mH
Filter Capacitance	25 μH
SAF Inductor	438 μH
SAF DC capacitor	2800 μF
DC bus voltage	700 V
No. of Solar cells	320*36
PV Nominal Voltage	48 V
PV Nominal Power	10 KW
PV Nominal Current	142 A

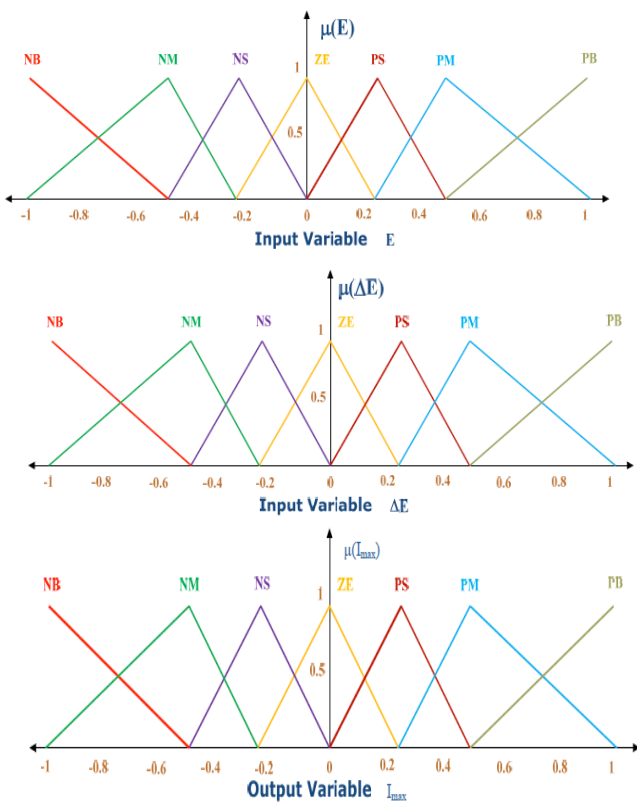


**Fig.9.** Membership function for variable E, CE and output

**Case A: balanced and unbalanced load**

To analysis the performance of the proposed system under balanced load conditions, the harmonic current detection block detects the variation of the supply current as soon as it occurs and it generates the actuating signal to activate the PWM pulse generator. The supply current is the sum of load current and injected SAF output current. During the initial period, there is no load deviation in the load. Hence, the programmable three-phase AC voltage source feeds the total active power of 1000 W to the load.

During the transient, three-phase load is reduced to two phases between 0.1 and 0.2s. The load is changed to two phase load and also the load currents are absent between 0.2 s and 0.25 s. These loads are applied again at 0.25 s respectively as shown in Fig.10a. It's observed From Fig.10b. The SAF responds to inject the compensating current in shunt with the supply to restore the source current at nominal level as shown in Fig.10c. It reduces the supplied active power of source from 1000 W to 520 W as shown in Fig. 11. The resultant active power of the load oscillates at 0.1 sec and it stabilizes at 0.13 sec. During the period, the reactive power supplied by the source is reduced from 600 VAR to 210 VAR. The SAF responds to the current transient and injects a reactive power of 400 VAR to restore the reactive power of the load. Neutral current during load changes as shown in Fig.12. The harmonics spectrum with and without the controller as shown in Fig.13.

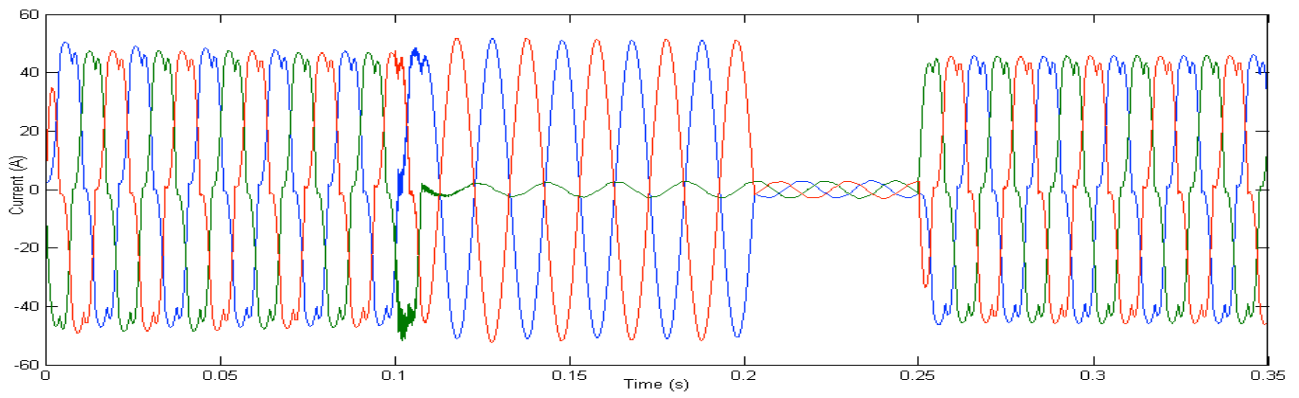


Fig.10a. load current without compensation.

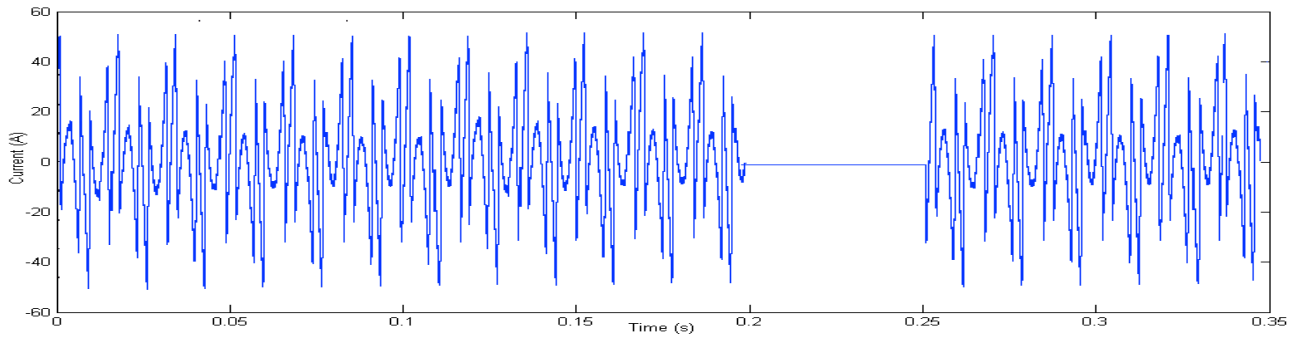


Fig.10b. Injected current for compensation.

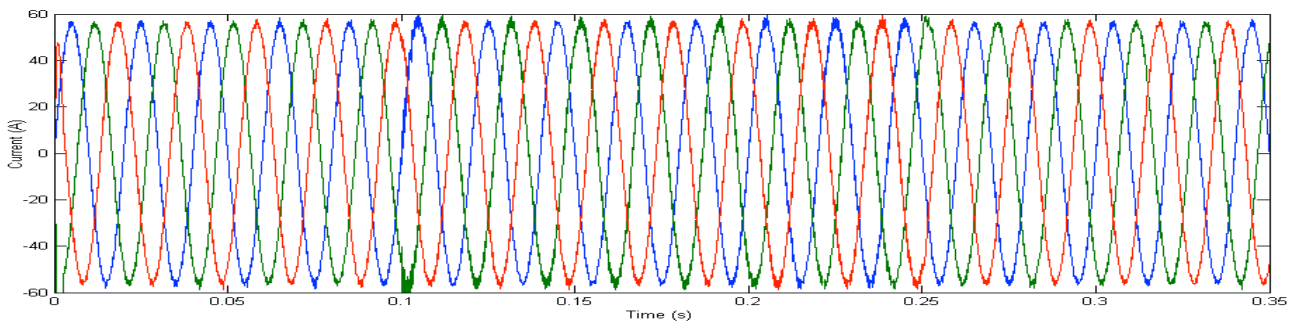


Fig.10c. Source current after compensation.

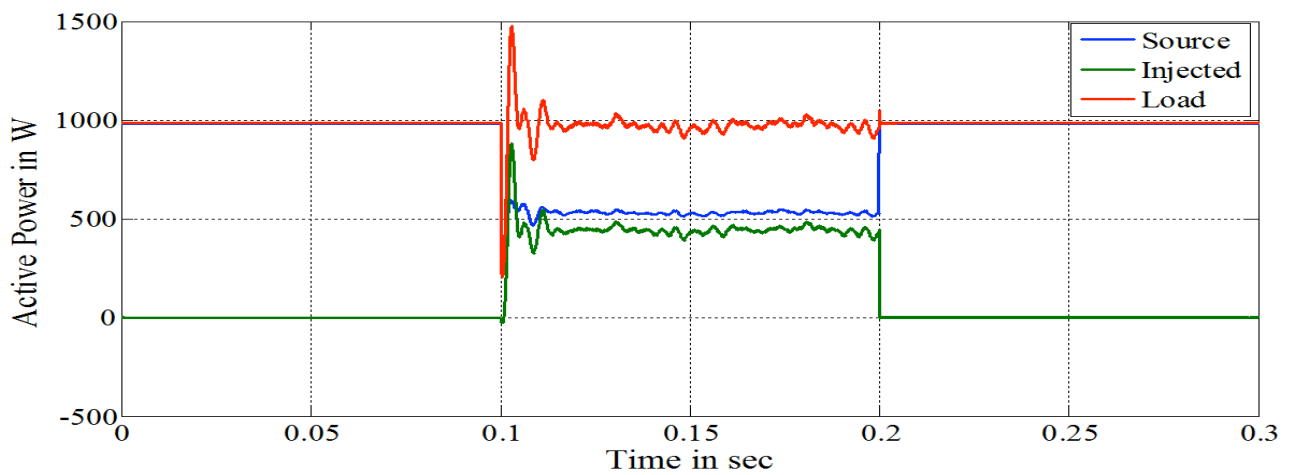


Fig.11. Source, injected and load reactive power at 50% of unbalanced Source voltage

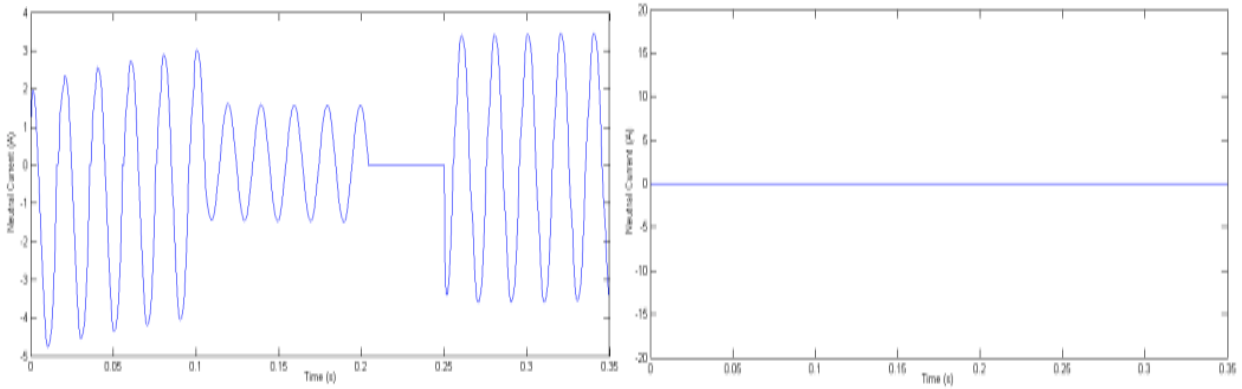


Fig.12. Neutral current compensation without and with SAF.

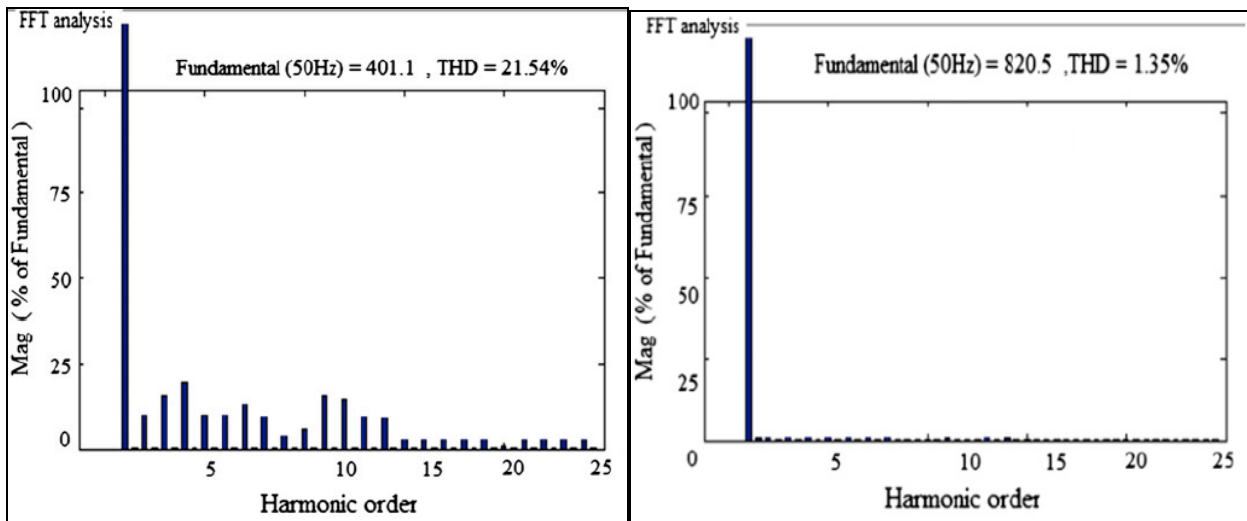


Fig.13. Phase A current THD spectrum before and after compensation

**CASE B: Energy Conservation**

The PV system is simulated with 5 number of 200W PV modules produce a total voltage and power of 60 V and 1000 W, respectively. Fig.14. shows the voltage, current and power at maximum power point which is being tracked by fuzzy MPPT controller at different temperature and constant irradiation conditions. Fig.15. shows the response time of two MPPT controllers. At standard test condition i.e. at irradiation of 1000 Watt/m<sup>2</sup> and temperature of 25<sup>0</sup> C the P&O MPPT controller is taking 0.1676 seconds to track the maximum power point whereas the fuzzy MPPT controller is taking only 0.0122 seconds to track the maximum power point. It concludes that the fuzzy based MPPT controller can reduce the maximum power tracking time by 88.18% as compared to conventional perturb and observe based MPPT controller. When the power generation on the PV system is greater than the load demand, then the coordinating logic presented in the Table 2, connects the output of the PV system to manage the load demand. The RMS value of the supply voltage, injected voltage and load voltage of the SAF for energy conservation mode are shown in Fig. 16.

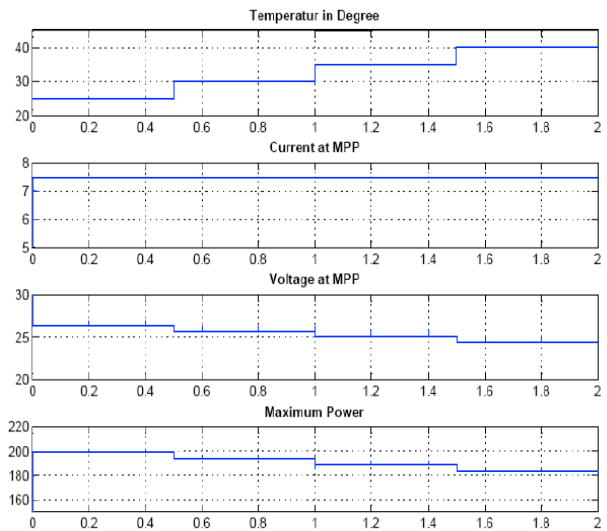


Fig.14. Simulation result of maximum current, voltage and power with Varying temperature and constant irradiation i.e. at 1000W/m<sup>2</sup> by fuzzy MPPT controller

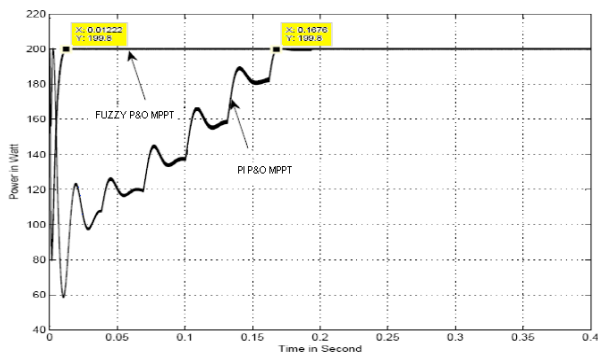


Fig.15. Single panel output by MPPT P&O Fuzzy Controller Method

In this case, the SAF injects the nominal voltage of 400 V in parallel with the load. On examining the results, it is found that the proposed SAF is able to conserve the energy. This case provides an additional financial benefit to the users by reducing the power consumption from the utility grid. The active and reactive powers of the SAF in energy conservation mode are shown in Fig.17.

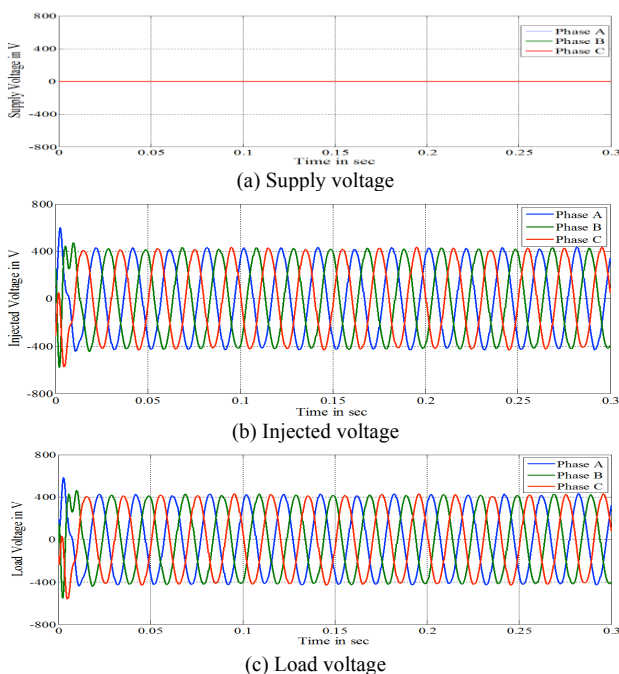


Fig.16. Supply injected and load voltage of the 3-phase PV-SAF

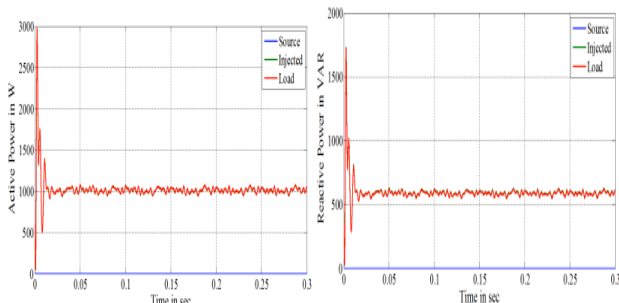


Fig.17. Active & reactive power of the PV-SAF

In this case, the SAF injects an active power of 1000 W and reactive power of 600 VAR to the load. The FFT analysis has been carried out to determine the THD, which is illustrated in the Table 7. It is observed that the proposed fuzzy controller based P&O MPPT controller tracked the maximum power generated by the PV array with 88.18 % of efficiency and also the proposed SAF ICC maintains the THD below 5% as per IEEE519 standards.

Table 7. THD comparison for two controllers

Simulation Results Comparison			
Three phase	Without SAF	With SAF	
		PI-ICosΦ	FLC-ICosΦ
Phase A THD %	21.54	8.38	2.39
Phase B THD %	22.40	8.50	2.53
Phase C THD %	20.90	8.42	2.40

8. Conclusion

This paper presents a novel application of utilizing a PV solar system as SAF for harmonic mitigation, reactive power compensation and neutral current compensation at the point of common coupling (PCC) at a small industry. A DC-DC converter with fuzzy controller based P&O MPPT algorithm is implemented to track the maximum power point of the PV array. A fast convergence with small oscillation at the maximum power point can be achieved by this method. This novel PV-SAF can reduce the energy consumption from the three phase utility grid, when the PV system generates excessive power or equal power to the load demand. Further, it reduces the energy consumption tariff and avoids the use of stabilizer for the individual equipment at a residence, small industry, etc. The simulation and experimental results shows that the PV-SAF performance is satisfactory in mitigating the current harmonics for the 24\*7 hours and reduces the THD level as per the IEEE519 standard.

Acknowledgment

Authors wish to thank Er.N.Ravichandran, A.E.E., MRT, Mettur Thermal Power Station (MTPS) and Mr.S.Manikandan M.E., Assistant Engineer, Numeric Power System, Chennai for provides technical information about generation, transmission and distribution of electrical power in southern grid, India.

References

1. El-Habrouk M & Darwish M.K, Active power filters: a review, *IEEE Proceedings on Electric Power Applications*, 5 (2000) 403-413.
2. Akagi Hirofumi, Kanazawa, & Nabae Akira, Instantaneous reactive power compensators comprising switching devices without energy storage components, *IEEE Transactions on Industry Applications*, 20 (1984) 625-630.

3. Mikkili S & Panda A K, Instantaneous Active and Reactive Power and Current Strategies for Current Harmonics Cancellation in 3-ph 4Wire SHAF with Both PI and Fuzzy Controllers, *Journal of Energy and Power Engineering*, 3 (2011) 285-298.
4. Salmeron P & Herrera R S, Distorted and Unbalanced Systems Compensation within Instantaneous Reactive Power Framework, *IEEE Transactions on Power Delivery*, 21 (2006) 1655-1662.
5. Bhuvanewari G. & Nair M G, Design, Simulation, and Analog Circuit Implementation of a Three-Phase Shunt Active Filter using the ICos $\Phi$  Algorithm, *IEEE Transactions on Power Delivery*, 23 (2008) 1222-1235.
6. Tamilnadu Agriculture Weather Network (TNAU). Coimbatore, India. (<http://tawn.tnau.ac.in/action?action=lastMonthReport&block=47&district=6.>), 2013.
7. Altas H & Sharaf A M. A photovoltaic array simulation model for MATLAB simulink GUI environment. *Proc. of Clean Electrical Power Conference '07*, (2007) 341-345.
8. El-Tayyan AA, PV system behavior based datasheet, *J. of Electron Devices*, 9 (2011) 335-341.
9. Mohan N & Undeland T M, *Power Electronics Converters: Applications and Design* (Third Edition, Jhon Wiley & Sons Asia Pte. Ltd., Singapore), 2006.
10. Elgendy M A & Zahawi B, Assessment of perturb and observe MPPT algorithm implementation techniques for PV pumping applications, *IEEE Transaction on Sustainable Energy*, 3 (2012) 21-33.
11. Jain S K, Fuzzy Logic Controlled Shunt Active Power Filter for Power Quality Improvement, *IEEE Proceedings Electric Power Applications*, 149 (2002) 317-328.
12. Kirawanich P & O'Connell R M, Fuzzy Logic Control of an Active Power Line Conditioner, *IEEE Transactions on Power Electronics*, 19 (2004) 1574-1585.